

Full Length Research Paper

Optical digital sensor for three-dimensional turbulent flow visualization

Maged Marghany* and Mazlan Hashim

Institute of Geospatial Science and Technology (INSTeG), University Teknologi Malaysia,
81310 UTM, Skudai, Johore Bahru, Malaysia.

Accepted 19 January, 2011

The Nikon Coolpix885® conventional digital camera is utilized to reform three-dimensional (3-D) turbulent pattern on lake that is situated in University Technology Malaysia (UTM). The main objective of this study is to use fuzzy arithmetic to reduce the errors arising from noise in digital camera data when constructing turbulent pattern flow. In doing so, the fuzzy B-spline algorithm, which assemble a global topological between the data points, are used to support an approximation to the real surface. Further, the fuzzy B-spline is performed to water surface information which estimated from 2-D digital camera images.

Key words: Digital camera, turbulent flow, fuzzy B-spline, three-dimensional (3D) reconstruction.

INTRODUCTION

Turbulent flow is considered to provide key parameters for coastal engineering, coastal navigation and civil structures engineering designing. The turbulent flow information in small-scale such as narrow channels and large-scale zones such as coastal zone or rivers is valuable for economical, security and marine environmental protection. The mathematical model is not acceptable to provide perfect description for turbulent flow. Researchers agreed that turbulent flow is governed by the conversation of mass and momentum. Therefore, researchers have implemented the Navier-Stockes equations to describe the complexity of turbulent flow. The Navier-Stockes equations, nevertheless cannot be solved analytically because of misgivings, and the regularity of solutions of these equations is established rigorously (Bohr et al., 1998). Consequently, remote sensing techniques have potential to track the spatial variation of turbulent flow in the ocean or in the estuary. Nevertheless, satellite remote sensing data are not able to track coastal turbulent flow over the short period of few hours due to their motion along the outer space (Maged

and Mazlan, 2006). For instance, for each LANDSAT-4 and -5 satellite, the orbit repeat cycle is 16-day. Further, the repeat period for JERS-1 and ALOS was 44 days. In contrast, RADARSAT-1 SAR provides 1-day repeat coverage over the Arctic and approximately 3-day repeat coverage at midlatitude (Lillesand et al., 2004). In this study, we address the question using low cost optical sensor such as a digital camera for turbulent flow in narrow water channel. Nevertheless, the concept of using a conventional imaging camera as a remote sensing instrument is not unknown (Goddijn-Murphy et al., 2009). Goddijn-Murphy et al. (2009) reported that an airborne standard 35 mm camera was used to study the frontal in a coastal zone as shown in study of Figueiredo et al. (2001). Further, Dugan and Piotrowski (2003) have modeled sea surface current which is based on Doppler shift of gravity waves that acquired from airborne digital camera. Recently, Goddijn-Murphy et al. (2009) used the conventional digital camera of the Nikon Coolpix885® and the SeaLife to find out the physical properties the water quality. In this context, Goddijn-Murphy et al. (2009) estimated water quality parameters based on the digital values of RGB ratio images. The contribution of this work is to utilize fuzzy B-spline for 3D turbulent flow visualization from the conventional digital camera with fix slanting angle of 40°. Two hypothesis are examined:

*Corresponding author. E-mail: maged@utm.my, magedupm@hotmail.com.

- (i) The conventional digital camera can be used to imagine turbulent flow in narrow channel.
- (ii) Fuzzy B-spline can be used to reconstruct 3-D of turbulent flow from two dimensional image without any requirement for any digital elevation points.

Under these circumstances, Maged et al. (2010) imposed fuzzy B-spline with Volterra algorithm for 3D bathymetry reconstruction from Airborne TOPSAR polarized data. Maged et al. (2010) reported that fuzzy B-spline algorithm provides a clear discrimination between smooth and rough bathymetry. In consequence, Annel et al. (1997), Rövid et al. (2004) and Maged et al. (2010) agreed that fuzzy B-spline algorithm can distinguish between smooth and jagged surfaces. In fact, fuzzy B-spline involves triangle-based criteria and edge-based criteria. Such parameters provide high-quality visualization in computer graphics (Annel et al., 1997).

EXPERIMENTALS

Image acquisition

Optical image data acquired using The Nikon Coolpix885@ conventional digital camera. These data contain Red (R), Green (G), and Blue (B) bands. According to Goddijn-Murphy et al. (2009) the Nikon Coolpix885 digital camera can adjust colours according to the colour of the lighting environment so those colours that appear white to the human eye also appear white when viewed in the final picture. Following Goddijn-Murphy et al. (2009), the camera used in the manual white balance setting 'direct sunlight' which is known as "white balance". In fact, a changed white balance setting changed the observed colour ratios. In this context, it is an essential to maintain the digital camera in a fixed white balance setting. Further, from each picture, the RGB values of the visible image of the projected beam derived, quantifying the response of the three bands to light of a certain wavelength. An experiment using the CP885, in which a sheet of uniform blue colour containing different sized black areas imaged, showed RGB values of the blue section did not change with the size of the black fraction. It is, therefore, assumed that the effects of white balancing are similar for the camera used *in situ*, and for the spectrophotometer measurements and that the same is applied to the ECOshot. Different exposure compensation values did not relate to different response values and one picture per wavelength was taken using zero exposure compensation value, 0 eV. For the CP885, this achieved by using a 1 s exposure time, and aperture setting f/2.8 (Goddijn-Murphy et al., 2009).

The CP885 is mounted on camera holder away from the wanted target with 10 m with 1 m elevation and view oblique angle of 40°. The selected view angle is considered appropriate view to capture the picture of water flow. The experiment is implemented to lake that is located at University Technology Malaysia (UTM). The images are taken every 10 min and then transferred to digital number for easy of processing using fuzzy B-spline algorithm.

The fuzzy B-splines method

The fuzzy B-splines (FBS) are introduced allowing fuzzy numbers

instead of intervals in the definition of the B-splines. Typically, in computer graphics, two objective quality definitions for fuzzy B-splines are used: triangle-based criteria and edge-based criteria. Indeed, triangle-based criteria are a function of angles and lengths while edge-based criteria are based on region boundaries and edges are closely related (Annie et al., 1995). A fuzzy number is defined using interval analysis. There are two basic notions that we combine together: confidence interval and presumption level. A confidence interval is a real values interval which provides the sharpest enclosing range for current gradient values. An assumption level μ -level is an estimated truth value in the (0, 1) interval on our knowledge level of the gradient current (Anile et al., 1995). The 0 value corresponds to minimum knowledge of digital number variations in digital camera, and 1 to the maximum digital values. A fuzzy number is then prearranged in the confidence interval set, each one related to an assumption level $\mu \in (0, 1)$. Moreover, the following must hold for each pair of confidence intervals which define a number: $\mu \succ \mu' \Rightarrow d \succ d'$. Let us consider a function $f: d \rightarrow d'$, of N fuzzy variables d_1, d_2, \dots, d_n . Where d_n are the global minimum and maximum values of digital number spatial variations. Based on the spatial variation of the digital number, the fuzzy B-spline algorithm is used to compute the function f . According to Anile et al. (1997), an assumption level μ can be express by

$$\mu(d): d \rightarrow [0, 1] \quad (1)$$

The input d (digital number) are fed into fuzzy rule base to formulate based on fuzzy deductive reasoning. This step involves function f , logical operation and if-then rules.

Following Maged and Mazln (2006), the construction begins with the digital value of turbulent flow in a fixed kernel window size of 512×512 pixels and lines is considered as a triangular fuzzy number defined by a minimum, maximum and measured value (Maged et al., 2007). Among all the fuzzy numbers falling within a kernel window size, a fuzzy number is defined whose range is given by the minimum and maximum values of gradient of turbulent flow's digital numbers along each kernel window size. Furthermore, the identification of a fuzzy number is acquired to summarize the digital number values in a cell and it is characterized by a suitable membership function. The choice of the most appropriate membership is based on triangular numbers which are identified by minimum, maximum, and mean digital values of turbulent flows which are acquired from digital camera (Russo, 1998; Rövid et al., 2004; Maged et al., 2010).

RESULTS AND DISCUSSION

Figure 1 shows the composite color image of RGB where the turbulent flow is dominated by bright spot pixels compared with surrounding water flow pixels. Because of, the digital camera has fundamentally three-band radiometers, with bands centred on wavelengths in the red, green and blue parts of the visible spectrum. The bands are, similar to human vision, broad and largely overlapping. This result confirms the study of Goddijn-Murphy et al. (2009).



Figure 1. Composite color image derived from the Nikon Coolpix885.

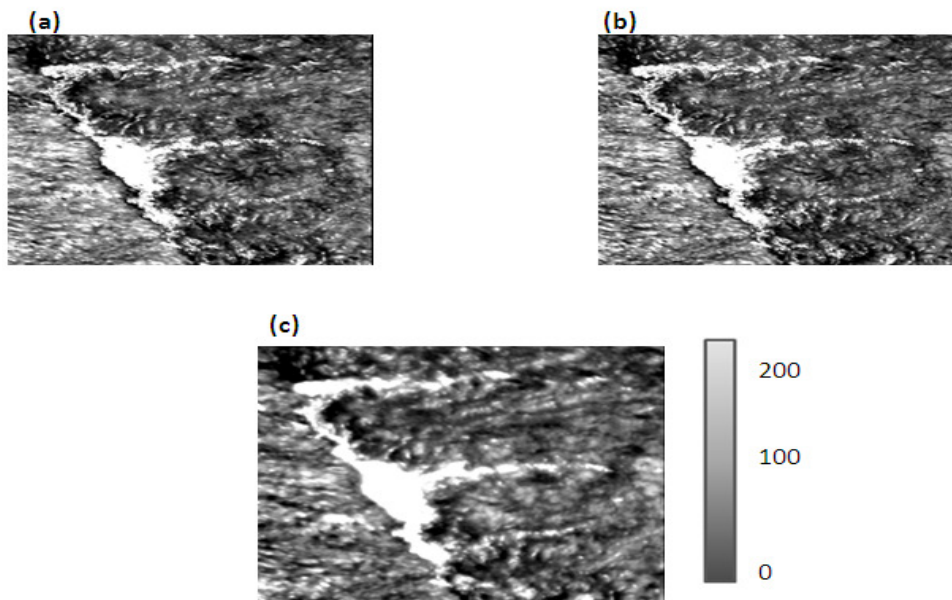


Figure 2. Grey level variations for (a) Red; (b) Green; (c) Blue bands.

This can be clearly observed by high DN (Digital Number) value of 255 for blue color as compared to R and G (Figure 2). Blue band (B) shows sharpness boundary

between turbulent flow and surrounding water flow pixels. The maximum DN value of 255 is found with Blue band as compared to Red and Green bands. In reality, Blue band

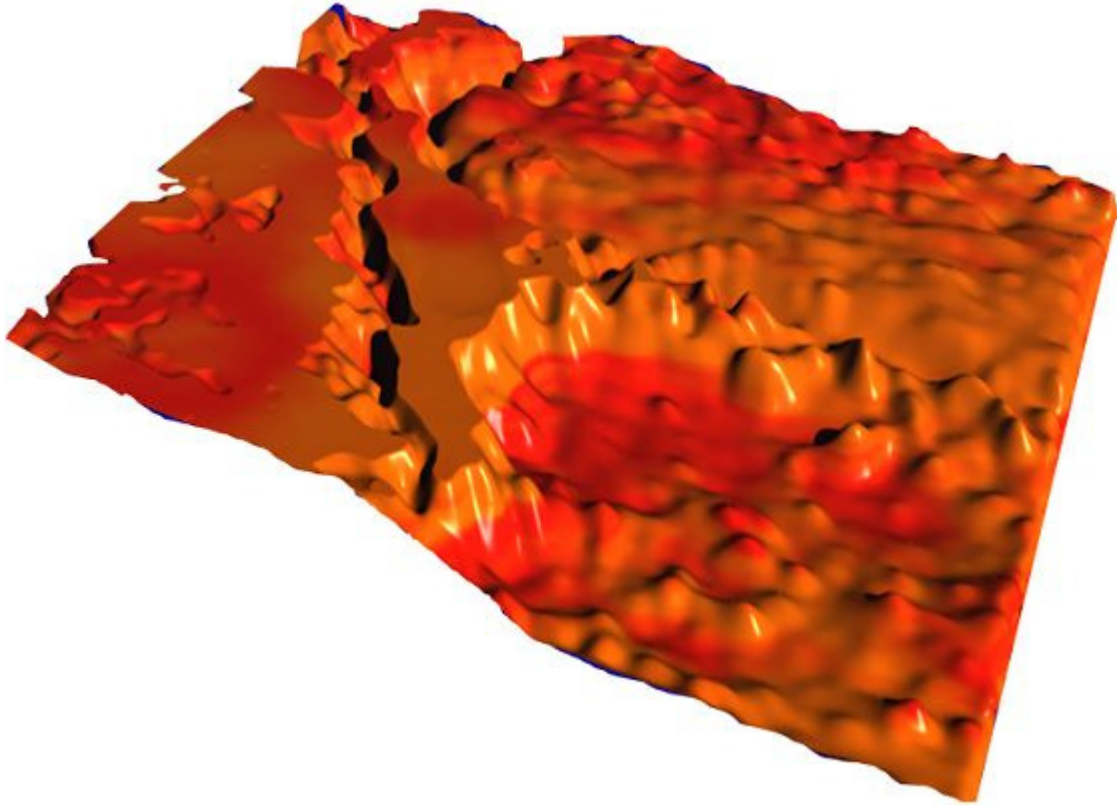


Figure 3. 3D fuzzy B-spline visualization.

has narrower band widths, enabling the finer spectral characteristics of the targets to be captured by the sensor. Further, the reflectance of clear water is generally low. However, the reflectance is maximum at the blue end of the spectrum and decreases as wavelength increases. Clearly, the Blue band can capture high reflectance energy of the turbulent flow compared with Red and Green bands. Fundamentally, the energy of a photon is inversely proportional to the wavelength. In consequence, Blue band has smaller wavelength of 450 nm which the smallest among Red and Green bands (Figueiredo et al., 2008; Maged and Hashim, 2010).

The result of fuzzy B-spline algorithm is shown in Figure 3. It is clear that the 3D visualization discriminates between different flow patterns. Figure 3 shows clearly the irregular water pattern flow as indicator for turbulent movement. Further, the boundary between laminar and turbulent flow can be distinguished (Figure 3).

It is clear that involving of fuzzy B-spline in 3-D turbulent flow visualization has produced real visualization. Therefore, the visualization of 3-D turbulent flow is sharp due to the fact that each operation on a fuzzy number becomes a sequence of corresponding operations on the respective μ -levels, and the multiple occurrences of the same fuzzy parameters evaluated as a result of the function on fuzzy variables. In addition, the fuzzy B-spline

depicts optimize a local triangulation between two different points (Anile et al., 1995). This corresponds to the feature of deterministic strategies of finding only sub-optimal solutions which usually overcomes uncertainties. In this context, the spatial cluster of gradient flow at each triangulation points can be simulated (Figure 3). Consequently, triangle-based criteria follow the rule of maximization or minimization, respectively, of the angles of each triangle (Fuchs et al., 1997) which prefers short triangles with obtuse angles. Further, edge-based criteria prefer edges that are closely related. This study confirms the previous studies of Anile et al. (1995), Fuchs et al. (1977), Dean et al. (2000), Maged et al. (2010). Indeed, these studies have agreed that fuzzy B-spline algorithm is an accurate tool for 3-D surface reconstruction from 2-D data.

Conclusions

This work has demonstrated a new method to utilize the Nikon Coolpix885@ conventional digital camera for 3-D turbulent visualization. In doing so, fuzzy B-spline algorithm is implemented to reconstruct 3-D water flow from 2-D image that is derived from the Nikon Coolpix885@ conventional digital camera. Consequently, it

is easy to discriminate between a rough surface flow structures and smooth surface flow. In fact, the fuzzy B-splines are considered as deterministic algorithms which are described here to optimize a triangulation only locally between two different points. In addition, fuzzy B-spline algorithm is able to keep track of uncertainty and provide tool for representing spatially clustered gradient flow points. In conclusion, the fuzzy B-spline algorithm can be used for 3-D turbulent flow reconstruction without existence of any information regarding water or topography elevation.

REFERENCES

- Anile AM, Deodato S, Privitera G (1995). Implementing fuzzy arithmetic, *Fuz. Set. Syst.*, 72: 123-156.
- Anile AM, Gallo G, Perfilieva I (1997). Determination of Membership Function for Cluster of Geographical data. Genova, Italy: Institute for Applied Mathematics, National Research Council, University of Catania, Italy, Oct. 1997. Tech. Rep., 26/97: 1-25.
- Bohr T, Jensen MH, Paladin G, Vulpiani A (1998). *Dynamical Systems Approach to Turbulence*. Cambridge University Press.
- Dean C, Warner TA, McGraw JB (2000). Suitability of the DSC460c colour digital camera for quantitative remote sensing analysis of vegetation. *ISPRS J. Photogramm.*, 55: 105-108.
- Dugan JP, Piotrowski CC (2003). Surface current measurements using airborne visible time series. *Rem. Sens. Environ.*, 84: 309-319.
- Figueiredo dSJ, Duck RW, Anderson JM, McManus J, Monk JGC (2001). Airborne observations of frontal systems in the inlet channel of the Ria de Aveiro, Portugal. *Phys. Chem. Earth, B* (26): 713-719.
- Fuchs H, Kedem ZM, Useton SP (1997). Optimal Surface Reconstruction from Planar Contours. *Commun. ACM*, 20: 693-702.
- Goddijn-Murphy LD, Dailoux MW, Bowers D (2009). Fundamentals of in situ digital camera methodology for water quality monitoring of coast and ocean. *Sens.*, pp. 5825-5843.
- Lillesand TM, Kiefer RW, Chipman JW (2004). *Remote sensing and Image interpretation*. 4th edition, John Wiley & Sons, USA.
- Maged M, Hashim M (2006). Three-dimensional reconstruction of bathymetry using C-band TOPSAR data. *Photo. Fern. Geoin.*, S6: 469-480.
- Maged M, Hashim M (2010). MODIS satellite data for modeling chlorophyll-a concentrations in Malaysian coastal waters. *Int. J. Phys. Sci.*, 5(10): 1489-1495.
- Maged M, Hashim M, Cracknell AP (2007). 3D Bathymetry Reconstruction from AIRBORNE TOPSAR Polarized Data. In: Gervasi, O and Gavrilova, M (Eds.): *Lecture Notes in Computer Science. Computational Science and Its Applications – ICCSA 2007, ICCSA 2007, LNCS 4705, Part (I) 4707/2007*, Springer-Verlag Berlin Heidelberg, 2007: 410–420.
- Maged M, Mansor S, Hashim M (2009). Geologic mapping of United Arab Emirates using multispectral remotely sensed data. *Am. J. Eng. Appl. Sci.*, 2: 476-480.
- Maged M, Mazlan H, Cracknell AP (2010). 3-D visualizations of coastal bathymetry by utilization of airborne TOPSAR polarized data. *Int. J. Dig. Earth.*, 3(2): 187–206.
- Rövid A, Várkonyi AR, Várlaki P (2004). 3D Model estimation from multiple images." *IEEE International Conference on Fuzzy Systems, FUZZ-IEEE'2004*, July 25-29, 2004, Budapest, Hungary, pp. 1661-1666.
- Russo F (1998). Recent advances in fuzzy techniques for image enhancement. *IEEE Trans. Inst. Meas.*, 47: 1428-1434.